

Wettability effects on two- and three-fluid relative permeabilities

Scott A. Bradford ^{a,*}, Linda M. Abriola ^a, Feike J. Leij ^b

^a *University of Michigan, Department of Civil and Environmental Engineering, 181 EWRE, 1351 Beal Avenue, Ann Arbor, MI 48109-2125, USA*

^b *US Salinity Laboratory, US Department of Agriculture, Agricultural Research Service, 450 W. Big Springs Road, Riverside, CA 92507-4617, USA*

Received 30 August 1996; revised 26 January 1997; accepted 26 January 1997

Abstract

Specification of relative permeability (k_r)–saturation (S) relations for all fluid phases is required for the simulation of multiphase flow and transport in porous media. Indirect methods are frequently employed to estimate these k_r – S relations owing to the time, expense, and difficulty associated with direct measurements. A common indirect approach uses capillary pressure data in conjunction with a selected pore-size distribution model to estimate k_r – S relations. Such methods typically assume perfect wettability of the solid. Natural porous media, however, are composed of a variety of mineral constituents with different adsorptive properties, which can exhibit non-zero contact angles and/or fractional wettability. Consequently, fluid distributions in natural media may be more complex than those predicted by simple pore-size distribution models and, under such conditions, current estimation approaches for k_r may be inadequate. In this work, the pore-size distribution model of N.T. Burdine (1953, Relative permeability calculations from pore-size distribution data. Transactions of the American Institute of Mining, Metallurgical and Petroleum Engineers 198, 71–77) is extended to incorporate wettability variations. In this model, wetting and less wetting (non-wetting or intermediate) fluid pore classes are used to calculate k_r for water or organic. The wettability of the porous medium is used to determine the contributions of the pore classes to k_r . For both two- and three-fluid systems, the model predicts that an increase in the contact angle (measured through water) or organic-wet fraction of a medium will be accompanied by an increase in the water k_r and a decrease in the organic k_r . In three-fluid media, k_r values for water and organic depend on both liquid saturations when the solid is imperfectly wetted. The model assumes that wettability variation has no influence on the air k_r .

* Corresponding author. Tel.: +1 313 936 3175; fax: +1 313 763 2275; e-mail: sbrad@engin.umich.edu

Model predictions are shown to be consistent with available experimental data. © 1997 Elsevier Science B.V.

Keywords: Relative permeability; Wettability; Multiphase flow; Hydraulic properties

1. Introduction

The release of slightly miscible organic liquids to the subsurface environment poses a significant threat to soils and groundwater. To reliably predict the temporal and spatial distribution of such contaminants with multiphase flow and transport models, accurate estimates of capillary pressure (P_c)–saturation (S)–relative permeability (k_r) relations are required (Demond et al., 1996). The measurement of two- and, especially, three-fluid relative permeabilities, however, is difficult, time consuming, and expensive (Honarpour et al., 1986; Klute and Dirksen, 1986). Consequently, indirect approaches are frequently used to estimate k_r – S relations from more easily measured P_c – S data.

One indirect technique for obtaining k_r – S relations is based on an extension of the hydraulic radius concept (Carman, 1937) to multiphase systems (Rapoport and Leas, 1951; Morrow, 1970). A second approach uses statistical pore-size distribution models to predict the permeability relations (e.g. Burdine, 1953; Mualem, 1976; and Lenhard and Parker, 1987). These indirect approaches, however, have been limited in their development and application to perfectly wetted porous media. The hydraulic radius approach has not been used to predict k_r – S relations for systems of other wettabilities owing to the lack of reliable experimental methods or estimation procedures to obtain values of the interfacial areas that are required by this model. Statistical pore-size distribution models employed to date implicitly assume a distinct order of wettability.

The contact angle (ϕ) is often used for quantifying the wettability (the distribution of immiscible fluids near a solid) of porous media. For organic (o)–water (w)–solid (s) systems, the angle is typically measured after a drop of the organic liquid is placed on a flat solid that is immersed in water. Flat polished plates of silica or quartz are used to represent sandstone, while calcite is used if carbonates are prevalent (Anderson, 1986). The horizontal force balance equation for this system, Young's equation, defines the contact angle measured through water as:

$$\cos(\phi_{\text{sow}}) = \frac{\sigma_{\text{so}} - \sigma_{\text{sw}}}{\sigma_{\text{ow}}} \quad (1)$$

where σ is the interfacial tension (N m^{-1}) and the subscripts indicate the phases. When $\phi_{\text{sow}} < 90^\circ$ water is the wetting fluid, whereas, for $\phi_{\text{sow}} > 90^\circ$ the water is the non-wetting fluid; the converse occurs for the organic.

The microscopic contact angle defined by Eq. (1) will vary spatially in natural porous media owing to contaminant aging (Powers and Tamblin, 1995), and/or variations in aqueous chemistry (Demond et al., 1994), mineralogy (Anderson, 1987a), organic matter distributions (Dekker and Ritsema, 1994) and surface roughness (Morrow, 1975). When both water- and organic-wet sites are present, this condition is referred to as fractional

wettability. In the petroleum literature, fractional wettability has been recognized as a ubiquitous condition (Brown and Fatt, 1956; Donaldson et al., 1969; Salathiel, 1973). Hence, a single value for the contact angle measured on a flat polished solid is only a crude approximation for natural systems. Alternatively, capillary pressure data may be used to infer the average influence of wettability (Donaldson et al., 1969; Bradford and Leij, 1995a, Bradford and Leij, 1995b). Wettability effects on capillary pressure data have been observed to be either saturation dependent or independent for various fluid and solid properties (Donaldson et al., 1969; Morrow, 1976; Bradford and Leij, 1995a,b).

Two-fluid relative permeability relations are significantly affected by the solid's wettability (Anderson, 1987b; Honarpour et al., 1986). Research concerning the effects of wettability on k_r - S relations has been conducted by Fatt and Klikoff (1959), Donaldson and Thomas (1971), Owens and Archer (1971), Morrow et al. (1973), McCaffery and Bennion (1974), Heaviside et al. (1987) and Demond and Roberts (1993). These studies indicate that, for media containing organics and water, an increasing contact angle or organic-wet fraction is accompanied by an increase in the k_{rw} and a decrease in k_{ro} (i.e. Owens and Archer, 1971; Donaldson and Thomas, 1971; Heaviside et al., 1987). This observed change in relative permeability may be explained by considering the distributions of the fluids: water tends to reside in the smaller, less conductive, pores of water-wet media and in the larger pores of organic-wet media, with the converse true for the organic.

A number of previous studies have presented measured three-fluid k_r - S relations (Leverett and Lewis, 1941; Caudle et al., 1951; Corey et al., 1956; Reid, 1958; Snell, 1962; Donaldson and Dean, 1966; Sarem, 1966; Saraf and Fatt, 1967; Oak et al., 1990; and Dria et al., 1993). Donaldson and Kayser (1981) reviewed the early studies and found marked differences owing to experimental errors, simplifying assumptions, and wettability differences. Published data qualitatively demonstrate the significance of wettability and hysteresis on k_r - S relations (Honarpour et al., 1986). For example, water and oil relative permeabilities have been reported to be functions of their own saturation or both liquid saturations (e.g. Oak et al., 1990).

The simulation of multiphase flow and transport processes is likely limited by our ability to accurately characterize the hydraulic properties of the system. Recently, Demond et al. (1996) demonstrated that the use of inaccurate estimates of k_r - S relations results in dramatically different simulation predictions from those based on measured parameters. The primary objective of this study is to develop an approach to estimate the influence of wettability variations on two- and three-fluid relative permeability relations.

2. Theory

Throughout this paper effective saturations are employed as a measure of the pore space accessible for flow. Because wettability affects the "immobile" residual wetting fluid, the effective saturation will depend upon the medium wettability, in addition to the pore structure. Terminology employed in this work pertaining to effective saturations

under various medium wettability conditions is defined in the Appendix A. For the reader's convenience, a notation section is also included at the end of the paper.

2.1. Hydraulic radius

The permeability of sands has been found to be correlated with the hydraulic radius, r_h , of a medium (Carman, 1937). For single phase flow, r_h is defined as the ratio of the porosity (ϵ) to the solid surface area per unit bulk volume (A_s):

$$r_h = \frac{\epsilon}{A_s} = \frac{1}{A_s^*} \quad (2)$$

where A_s^* is the solid surface area per unit pore volume. The Carman–Kozeny equation relates permeability and hydraulic radius as:

$$k = \frac{\epsilon r_h^2}{C_k} = \frac{\epsilon}{C_k} \left[\frac{1}{A_s^*} \right]^2 \quad (3)$$

where C_k is the Kozeny constant which has been empirically established to have a value of approximately 5 for unconsolidated sand (Carman, 1937). Rapoport and Leas (1951) extended the hydraulic radius concept to two-phase flow by replacing: (i) ϵ with the "effective porosity" with respect to the fluid (ϵS); and (ii) A_s^* with the sum of the interfacial areas bounding a flowing fluid. According to their procedure (Rapoport and Leas, 1951) the two-fluid relative permeability to water is written as:

$$k_{rw}(\bar{S}_w^{ow}) = (\bar{S}_w^{ow})^3 \left[\frac{A_{se}^*}{A_{sw}^* + A_{ow}^*} \right]^2 \quad (4)$$

and the relative permeability to organic is given as (cf., Morrow, 1970):

$$k_{ro}(\bar{S}_w^{ow}) = (1 - \bar{S}_w^{ow})^3 \left[\frac{A_{se}^*}{A_{so}^* + A_{ow}^*} \right]^2 \quad (5)$$

where \bar{S} is the effective fluid saturation; the subscript on S (or \bar{S}) indicates the fluid to which the saturation pertains and the superscripts denote all fluids present in the medium. The solid–water, solid–organic, and organic–water interfacial areas per unit pore volume are given as A_{sw}^* , A_{so}^* , and A_{ow}^* , respectively, while A_{se}^* is the effective solid surface area per unit pore volume. Rapoport and Leas (1951) employed an effective solid surface area in place of A_s^* in Eq. (4) to account for the reduction in area owing to the presence of immobile residual wetting saturation (discontinuous wetting fluid films coating the solids) which occurs in multi-fluid systems. Hence, these researchers defined A_{se}^* as the contact area (per unit pore volume) of the mobile wetting phase and the solid + immobile residual wetting phase matrix.

Similar to Eqs. (4) and (5), the hydraulic radius approach may be extended to three-fluid relative permeabilities. For the most general case of a three-fluid fractional wettability medium, these are given as:

$$k_{rw}(\bar{S}_w^{aow}, \bar{S}_o^{aow}) = (\bar{S}_w^{aow})^3 \left[\frac{A_{se}^*}{A_{sw}^* + A_{ow}^* + A_{aw}^*} \right]^2 \quad (6)$$

$$k_{ro}(\bar{S}_w^{aow}, \bar{S}_o^{aow}) = (\bar{S}_o^{aow})^3 \left[\frac{A_{se}^*}{A_{so}^* + A_{ow}^* + A_{ao}^*} \right]^2 \quad (7)$$

$$k_{ra}(\bar{S}_w^{aow}, \bar{S}_o^{aow}) = (\bar{S}_a^{aow})^3 \left[\frac{A_{se}^*}{A_{sa}^* + A_{aw}^* + A_{ao}^*} \right]^2 \quad (8)$$

where A_{sa}^* , A_{aw}^* , and A_{ao}^* are the solid–air, air–water, and air–organic interfacial areas per unit pore volume, respectively.

The interfacial areas in Eqs. (4)–(8) depend on saturation, pore-size distribution, and medium wettability (Bradford and Leij, 1997). If the hydraulic radius approach is valid, and accurate values of the interfacial areas are available, Eqs. (4)–(8) should provide a means to predict wettability effects on the relative permeability relations. Recently, Bradford and Leij (1997) presented an approach to estimate two- and three-fluid interfacial areas for various medium wettabilities. Their approach is based upon the thermodynamic description of two-fluid capillarity presented by Morrow (1970), which relates the work required to change the fluid saturation (the area under the P_c – S curve) to changes in the interfacial areas. According to their procedure, when the contact angle is less than 90° , the values of $A_{ow}^* + A_{sw}^*$ (cf. Eq. (4)) and $A_{ow}^* + A_{so}^*$ (cf. Eq. (5)) at a given saturation decrease with increasing contact angle. Hence, according to Eqs. (4) and (5), both k_{rw} and k_{ro} will increase with increasing contact angle. This prediction, however, contradicts experimental observations of k_{ro} (Owens and Archer, 1971; McCaffery and Bennion, 1974). It is likely that A_{se}^* also depends on the medium wettability since the residual immobile wetting saturation also is a function of medium wettability (Morrow, 1990). Since there are no available techniques for the estimation of A_{se}^* , the hydraulic radius approach for the prediction of k_r – S relations was not considered further in this work.

2.2. Pore-size distribution model adaptation

Owing to the difficulties in estimating parameters for the hydraulic radius model, an alternative indirect technique was sought for the predictions of k_r – S relations. The Burdine (1953) pore-size distribution model was selected as a basis for this approach owing to the ability of this model to predict the relative permeability relations for a perfectly wetted porous medium (tested on data reported by Morrow and McCaffery (1978)); other commonly used pore-size distribution models (e.g. Muallem, 1976) predict higher wetting phase relative permeability values at a given saturation than the Burdine model. Modification of the Burdine model (Burdine, 1953) is presented below for the nonhysteretic case.

2.2.1. Two-fluid systems

The Burdine model views the porous medium as a tortuous bundle of parallel capillary tubes. The size distribution of these tubes is estimated from primary drainage P_c – S data according to (Laplace, 1825):

$$R(\bar{S}_w^{\text{ow}}) = \frac{2\sigma_{\text{ow}} \cos(\phi_{\text{sow}})}{P_{\text{ow}}(\bar{S}_w^{\text{ow}})} \quad (9)$$

where R is the radius of a capillary tube, and $P_{\text{ow}} = P_o - P_w$ is the capillary pressure. Flow in the i th capillary tube is described by the Hagen–Poiseuille equation as:

$$q_i = -\frac{R_i^2 \rho g}{8\mu} \frac{dH}{dz} \quad (10)$$

where q_i is the average volumetric flux per unit cross-sectional area, R_i is the radius of the i th capillary tube, ρ is the fluid density, g is the acceleration owing to gravity, μ is the fluid viscosity, and dH/dz is the hydraulic head gradient in the z direction. Summation of the contributions from all fluid-filled pores leads to an expression of the average flux in a porous medium. Equating this flux to Darcy's law yields the following expressions for the relative permeability (Burdine, 1953):

$$k_{\text{rw}}(\bar{S}_w^{\text{ow}}) = (\bar{S}_w^{\text{ow}})^2 \frac{\int_0^{\bar{S}_w^{\text{ow}}} R(x)^2 dx}{\int_0^1 R(x)^2 dx} \quad (11)$$

$$k_{\text{ro}}(\bar{S}_w^{\text{ow}}) = (1 - \bar{S}_w^{\text{ow}})^2 \frac{\int_{\bar{S}_w^{\text{ow}}}^1 R(x)^2 dx}{\int_0^1 R(x)^2 dx} \quad (12)$$

where the tortuosity of the flow path is empirically accounted for in Eqs. (11) and (12) by using the square of \bar{S}_w^{ow} and $\bar{S}_o^{\text{ow}} = 1 - \bar{S}_w^{\text{ow}}$, respectively. If $R(x)$ is replaced by Eq. (9), one can see that the estimates for k_r given by Eqs. (11) and (12) are independent of the magnitude of σ_{ow} and ϕ_{sow} , as long as σ_{ow} and ϕ_{sow} are independent of saturation. Note that Burdine's model assigns the water to the "smaller" pores (see Eq. (11)) and the organic liquid to the "larger" pores (see Eq. (12)) by varying the integration limits. This implicitly assumes that water is the wetting fluid and that the organic is the nonwetting fluid.

In many cases, the fluid does not reside exclusively in a single pore class, as assumed by existing pore size distribution models. The literature suggests that fractional wettability porous media and, to a lesser extent, mineralogically homogeneous porous media exhibit spatially dependent wettability (i.e. Brown and Fatt, 1956; Morrow, 1975). For a given fluid pair, the filling sequence of pores is determined by the pore radius and pore wettability. Consequently, pore scale variability in wettability will influence the pores that are accessible for fluid flow. As the magnitude of the capillary pressure at a given saturation decreases, microscopic variations in wettability likely have a more pronounced effect on the pore filling sequence (McCaffery and Bennion, 1974).

Consider a two fluid, organic–water, porous medium system. Suppose that pores are divided into two classes (domains) by size, termed herein as “small” and “large”. In this system, the effective macroscopic wettability, as determined from P_c – S data, will determine the contribution of a given pore domain to the magnitude of k_r for each fluid. Based upon Eqs. (11) and (12), k_{rw} may be written as:

$$k_{rw}(\bar{S}_w^{ow}) = (\bar{S}_w^{ow})^2 \frac{[1 - f(\phi_{sow})] \int_0^{\bar{S}_w^{ow}} R(x)^2 dx + f(\phi_{sow}) \int_{1-\bar{S}_w^{ow}}^1 R(x)^2 dx}{\int_0^1 R(x)^2 dx} \tag{13}$$

where the first and second integrals in the numerator account for the contributions to the permeability of the smaller (water as wetting fluid) and larger (water as nonwetting fluid) pore domains, respectively. Similarly, k_{ro} is written as:

$$k_{ro}(\bar{S}_w^{ow}) = (1 - \bar{S}_w^{ow})^2 \frac{f(\phi_{sow}) \int_0^{1-\bar{S}_w^{ow}} R(x)^2 dx + [1 - f(\phi_{sow})] \int_{\bar{S}_w^{ow}}^1 R(x)^2 dx}{\int_0^1 R(x)^2 dx} \tag{14}$$

In Eqs. (13) and (14), $f(\phi_{sow})$ is an empirical weighting function which depends upon the macroscopic contact angle of the medium. Based upon available experimental evidence (McCaffery and Bennion, 1974), the following functional form is suggested:

$$f(\phi_{sow}) = \frac{1}{2} [1 - \cos(\phi_{sow})] \tag{15}$$

Here ϕ_{sow} is the effective macroscopic contact angle defined with respect to water as the “reference wetting fluid”. This contact angle may be either saturation independent or saturation dependent. When using $\phi_{sow}(\bar{S}_w^{ow})$, the values of k_{rw} and k_{ro} are determined at each saturation using a different weight.

Fig. 1 shows a plot of $f(\phi_{sow})$ when ϕ_{sow} is independent of saturation. The shape of $f(\phi_{sow})$ is such that increasing ϕ_{sow} leads to an increasing contribution of larger pores to

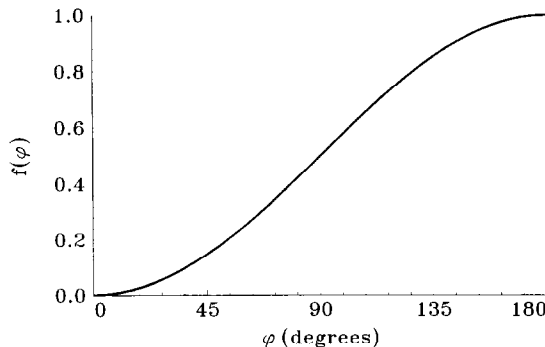


Fig. 1. Plot of weighting function (Eq. (15)), $f(\phi_{sow})$ verses ϕ_{sow} .

the determination of k_{rw} (see Eq. (13)); the converse occurs for k_{ro} (see Eq. (14)). Furthermore, observe that k_{rw} is uniquely determined by the smaller pores when $\phi_{sow} = 0^\circ$, equally determined by smaller and larger pores when $\phi_{sow} = 90^\circ$, and only determined by larger pores when $\phi_{sow} = 180^\circ$. According to Eq. (15), k_{rw} and k_{ro} are most sensitive to changes in ϕ_{sow} for $40^\circ < \phi_{sow} < 140^\circ$. McCaffery and Bennion (1974) found that k_{rw} and k_{ro} were relatively insensitive to changes in ϕ_{sow} when $\phi_{sow} < 49^\circ$ or $\phi_{sow} > 138^\circ$.

Scaling suggests that values of ϕ_{sow} , for a given porous medium, can be obtained from measured organic–water and air–organic P_c – S data and interfacial tensions, provided that $\phi_{sao} = 0^\circ$, using the following relation (Bradford and Leij, 1995a):

$$\cos(\phi_{sow}) = \frac{\sigma_{ao} P_{ow}(\bar{S}_w^{ow})}{\sigma_{ow} P_{ao}(\bar{S}_o^{ao})} \quad (16)$$

at points where $\bar{S}_w^{ow} = \bar{S}_o^{ao}$. A best fit value of ϕ_{sow} can be developed by considering a range of liquid saturations. Receding (ϕ_{sow}^R) and advancing (ϕ_{sow}^A) contact angles may be obtained by fitting P_c – S data for drainage and imbibition, respectively. A nonlinear least squares fitting procedure such as that of Marquardt (1963) can be used for this purpose. For systems having a saturation dependent wettability, values for $\phi_{sow}(\bar{S}_w^{ow})$ can be calculated at each saturation according to Eq. (16).

Many numerical multiphase flow simulators require simple closed-form analytical expressions for the relative permeability relations. Closed form expressions for the Burdine model (see Eqs. (11) and (12)) can be obtained when the model of van Genuchten (1980), with $m = 1 - 2/n$, is used to describe the P_c – S data. Analytical expressions for the modified Burdine's model can similarly be obtained.

2.2.2. Three-fluid systems

Pore-size distribution models similar to Eqs. (11) and (12) have also been developed to predict three-fluid relative permeability relations (Corey et al., 1956; Lenhard and Parker, 1987):

$$k_{rw}(\bar{S}_w^{aow}) = (\bar{S}_w^{aow})^2 \frac{\int_0^{\bar{S}_w^{aow}} R(x)^2 dx}{\int_0^1 R(x)^2 dx} \quad (17)$$

$$k_{ro}(\bar{S}_w^{aow}, \bar{S}_o^{aow}) = (\bar{S}_o^{aow})^2 \frac{\int_{\bar{S}_w^{aow}}^{\bar{S}_{il}^{aow}} R(x)^2 dx}{\int_0^1 R(x)^2 dx} \quad (18)$$

$$k_{ra}(\bar{S}_{il}^{aow}) = (1 - \bar{S}_{il}^{aow})^2 \frac{\int_{\bar{S}_{il}^{aow}}^1 R(x)^2 dx}{\int_0^1 R(x)^2 dx} \quad (19)$$

where \bar{S}_{il}^{aow} is the effective total liquid saturation ($\bar{S}_{il}^{aow} = \bar{S}_w^{aow} + \bar{S}_o^{aow}$). Note that even though multiple capillary pressure drops (P_{ow} and P_{ao}) occur in three-fluid systems the

same pore-size distribution is used in these models to characterize the permeabilities of the medium. The only difference between two- and three-fluid pore-size distribution models is the ‘‘assignment’’ of fluids to a pore domain, i.e. small and large for two-fluid systems compared with small, medium, and large for three-fluid systems. As for two-fluid systems, this is achieved by changing the integration limits.

To extend Eqs. (17)–(19) to account for various wettabilities, it is assumed herein that organic and water will be found in small and medium pore domains, and that air is restricted to the largest pore domain (air is always the non-wetting fluid). Based upon this assumption k_{rw} is determined by modifying Eq. (17) similar to Eq. (13):

$$k_{rw}(\bar{S}_w^{aow}, \bar{S}_o^{aow}) = (\bar{S}_w^{aow})^2 \frac{[1 - f(\phi_{sow})] \int_0^{\bar{S}_w^{aow}} R(x)^2 dx + f(\phi_{sow}) \int_{\bar{S}_o^{aow}}^{\bar{S}_w^{aow}} R(x)^2 dx}{\int_0^1 R(x)^2 dx} \quad (20)$$

where the limits of integration of the first and second integrals in the numerator assign water to the small and medium pore domains, respectively. Analogously, k_{ro} is determined by modifying Eq. (18) similar to Eq. (14):

$$k_{ro}(\bar{S}_w^{aow}, \bar{S}_o^{aow}) = (\bar{S}_o^{aow})^2 \frac{f(\phi_{sow}) \int_0^{\bar{S}_o^{aow}} R(x)^2 dx + [1 - f(\phi_{sow})] \int_{\bar{S}_w^{aow}}^{\bar{S}_o^{aow}} R(x)^2 dx}{\int_0^1 R(x)^2 dx} \quad (21)$$

The value of k_{ra} is obtained according to Eq. (19). The weighting function employed in Eqs. (20) and (21) is again given by Eq. (15). In this case, Eq. (15) is used to determine the contributions of the small and medium pore domains. Note again that, depending on fluid and solid properties, ϕ_{sow} may or may not be a function of saturation in Eq. (15). The value of ϕ_{sow} for air–organic–water systems can also be determined according to Eq. (16) since air is always (likely to be) the non-wetting fluid. This implies that ϕ_{sow} may be determined from the $P_{ow} - \bar{S}_w^{ow}$ or $P_{ow} - \bar{S}_w^{aow}$ relations because $P_{ow} - \bar{S}_w^{ow}$ data can be used to predict $P_{ow} - \bar{S}_w^{aow}$ relationships (Bradford and Leij, 1996).

3. Application

The equations described above for estimating wettability effects on two- and three-fluid $k_r - S$ relations require knowledge of the pore-size distribution and macroscopic contact angle of the porous medium. In the examples presented below, the pore-size distribution was estimated (Eq. (9)) from experimental primary drainage air–organic (Soltrol 220) $P_c - S$ data which were reported by Bradford and Leij (1995a). All porous media were composed of 25% very coarse sand, 50% coarse/medium sand, and 25% fine sand according to the USDA textural classification (Soil Survey Staff, 1975).

Table 1
Fluid and solid parameters

σ_{ao}	0.024 N m^{-1}
ϕ_{sao}	0°
S_{ro}^{ao}	$0.13 \text{ cm}^3 \text{ cm}^{-3}$
α	0.081 cm^{-1}
n	5.798

α and n are P_c – S model parameters (van Genuchten, 1980).

Table 1 lists the relevant fluid and solid parameters for this air–organic porous medium system (Bradford and Leij, 1995a). Hypothetical macroscopic contact angles were chosen to vary over a wide range of wetting conditions. Actual macroscopic contact angles can be fitted or calculated from P_c – S data and interfacial tensions according to Eq. (16). For simplicity, uniform and fractional wettability systems will be referred to herein as having saturation independent and saturation dependent contact angles, respectively.

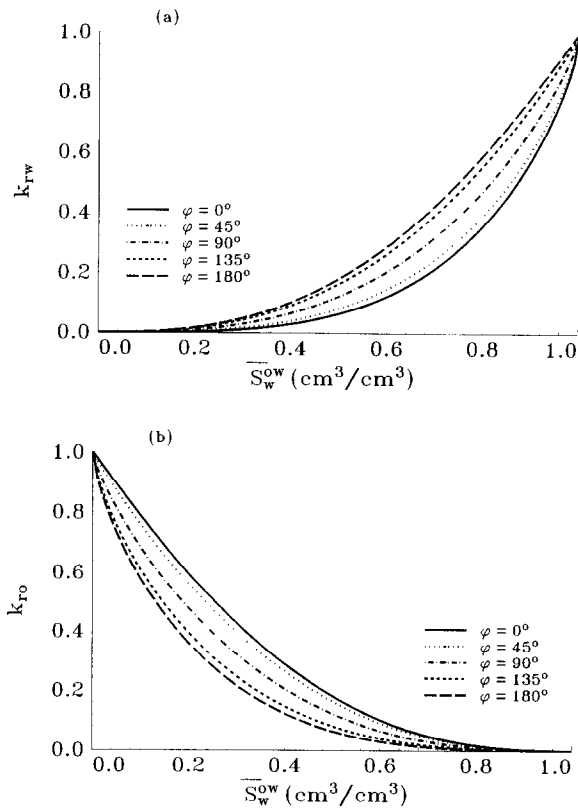


Fig. 2. (a) and (b). Estimated values of k_{rw} and k_{ro} according to Eqs. (13) and (14), respectively, for media having hypothetical ϕ_{sow} equal to 0° , 45° , 90° , 135° , and 180° .

3.1. Two-fluid systems

For the selected medium, Fig. 2(a) and Fig. 2(b) illustrate the predicted dependence of k_{rw} and k_{ro} (according to Eqs. (13) and (14), respectively) on a saturation independent contact angle. Note that an increasing ϕ_{sow} leads to an increase in k_{rw} and a decrease in k_{ro} . This result occurs owing to the change in roles (wetting versus non-wetting) of water and organic as ϕ_{sow} increases. These trends are consistent with the experimental results of Owens and Archer (1971) and McCaffery and Bennion (1974).

Fig. 3(a) shows the main imbibition fractional wettability $P_{ow}-S_w^{ow}$ relations (Bradford and Leij, 1995b) for media composed of 0, 25, 50, 75, and 100% organic-wet fractions: the octadecyltrichlorosilane (OTS) treated sand fraction. Fig. 3(b) shows values of $\phi_{sow}(\bar{S}_w^{ow})$ that were calculated according to Eq. (16) from these data, the air-organic P_c-S data given in Table 1, and the measured value of $\sigma_{ow} = 0.026 \text{ N m}^{-1}$ (Bradford and Leij, 1995a). Fig. 4(a) and Fig. 4(b) present the corresponding predictions

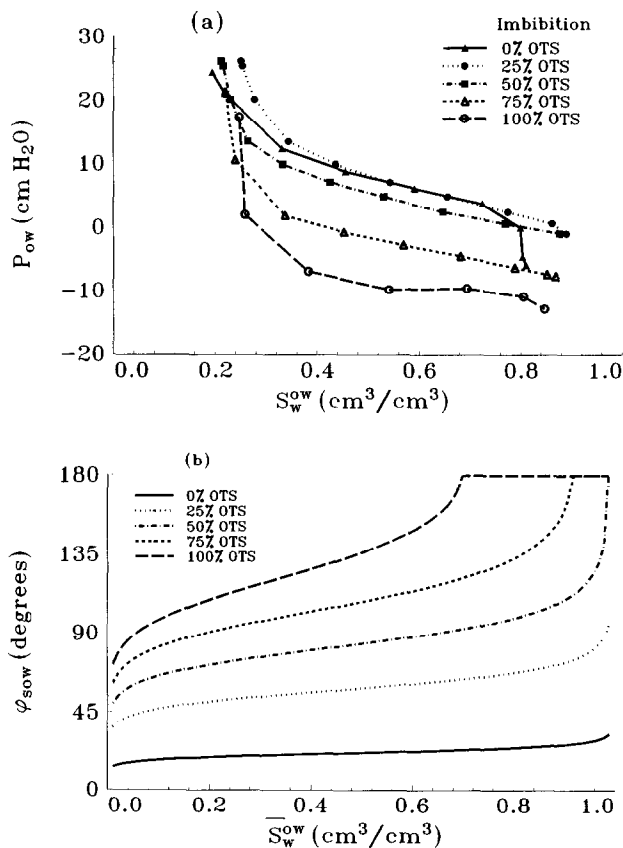


Fig. 3. (a) and (b). Measured main imbibition $P_{ow}-S_w^{ow}$ relations (Fig. 3(a)) and corresponding $\phi_{sow}(\bar{S}_w^{ow})$ relations (Fig. 3(b)) for fractional wettability media composed of 0, 25, 50, 75, and 100% organic-wet fractions (OTS).

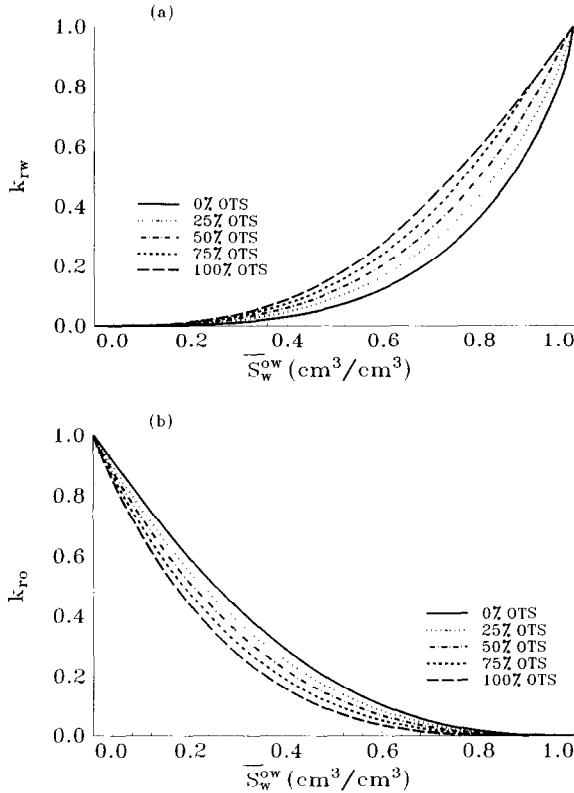


Fig. 4. (a) and (b). Calculated values of k_{rw} and k_{ro} according to Eqs. (13) and (14), using $\phi_{sow}(\bar{S}_w^{ow})$ in Eq. (15), for media composed of 0, 25, 50, 75, and 100% organic-wet fractions (OTS).

for k_{rw} (Eq. (13)) and k_{ro} (Eq. (14)), respectively. Note that increasing the organic-wet fraction leads to an increase in k_{rw} and a decrease in k_{ro} similar to reported experimental data (Donaldson and Thomas, 1971; Heaviside et al., 1987) and Fig. 2. In contrast to Fig. 2, calculated values of k_{rw} and k_{ro} here also depend on the $\phi_{sow}(\bar{S}_w^{ow})$ relation. In general, the saturation dependency of ϕ_{sow} was more pronounced for media with greater organic-wet fractions (see Fig. 3(b)).

3.2. Three-fluid systems

Predicted three-phase relative permeability dependence on contact angle is illustrated in Figs. 5 and 6. Fig. 5(a) and Fig. 5(b) present the functional dependence of the k_{rw} on \bar{S}_w^{aow} at fixed $\bar{S}_o^{aow} = 0.2$, and the functional dependence of k_{rw} on \bar{S}_o^{aow} at fixed $\bar{S}_w^{aow} = 0.4$ and 0.8, respectively, according to Eq. (20). Comparison of Fig. 5(a) and Fig. 5(b) reveals that k_{rw} is primarily a function of \bar{S}_w^{aow} since \bar{S}_w^{aow} determines the number of pores accessible for water flow. Fig. 5(b) shows that k_{rw} also depends on \bar{S}_o^{aow} as ϕ_{sow} increases, primarily at larger \bar{S}_w^{aow} . This is due to the influence of \bar{S}_o^{aow} on the

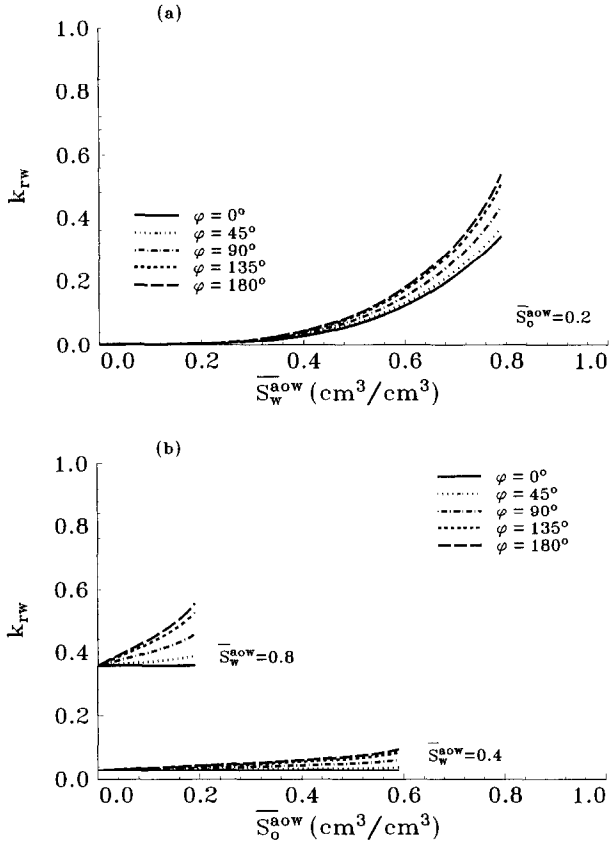


Fig. 5. (a) and (b). Calculated values of $k_{rw}(\bar{S}_w^{aoW})$ at fixed $\bar{S}_o^{aoW} = 0.2$, and $k_{rw}(\bar{S}_o^{aoW})$ at fixed $\bar{S}_w^{aoW} = 0.4$ and 0.8, respectively, according to Eq. (20) when ϕ_{sow} equals 0° , 45° , 90° , 135° and 180° .

configuration of water at larger contact angles. Note that a greater ϕ_{sow} increases $k_{rw}(\bar{S}_w^{aoW})$ (see Fig. 5(a)), in a similar manner as for two-fluid systems (see Fig. 2(a)), and also increases $k_{rw}(\bar{S}_o^{aoW})$ (see Fig. 5(b)). This result is consistent with the observations of Caudle et al. (1951), Reid (1958), Snell (1962), and Donaldson and Dean (1966) who found that k_{rw} depends on both \bar{S}_w^{aoW} and \bar{S}_o^{aoW} . Note that previous three-fluid pore-size distribution models are not able to produce such trends since they assume that k_{rw} is only a function of \bar{S}_w^{aoW} .

Fig. 6(a) and Fig. 6(b) present the functional dependence of the k_{ro} on \bar{S}_o^{aoW} at fixed $\bar{S}_w^{aoW} = 0.2$, and the functional dependence of k_{ro} on \bar{S}_w^{aoW} at fixed $\bar{S}_o^{aoW} = 0.4$ and 0.8, respectively, according to Eq. (21). Similar to the behavior of k_{rw} , observe that k_{ro} is mainly a function of \bar{S}_o^{aoW} (see Fig. 6(a)); \bar{S}_o^{aoW} determines the number of pores accessible for organic flow. The value of k_{ro} also depends on \bar{S}_w^{aoW} when $\phi_{sow} < 180^\circ$ (see Fig. 6(b)), primarily for large \bar{S}_o^{aoW} , since water affects the configuration of organic. Note that a greater ϕ_{sow} decreases $k_{ro}(\bar{S}_o^{aoW})$ (see Fig. 6(a)), in a similar manner as for

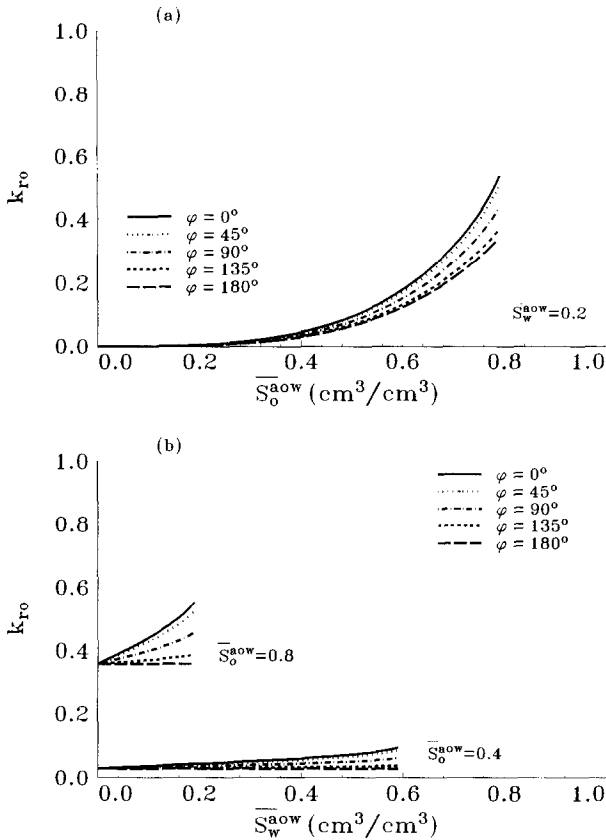


Fig. 6. (a) and (b). Calculated values of $k_{ro}(\bar{S}_o^{aoiw})$ at fixed $\bar{S}_w^{aoiw} = 0.2$, and $k_{ro}(\bar{S}_w^{aoiw})$ at fixed $\bar{S}_o^{aoiw} = 0.4$ and 0.8, respectively, according to Eq. (21) when ϕ_{soiw} equals 0°, 45°, 90°, 135° and 180°.

two-fluid systems (see Fig. 2(b)), and also decreases $k_{ro}(\bar{S}_w^{aoiw})$ (see Fig. 6(b)). Leverett and Lewis (1941), Caudle et al. (1951), Corey et al. (1956) were some of the first investigators to show that k_{ro} depended upon both \bar{S}_w^{aoiw} and \bar{S}_o^{aoiw} .

The three-phase relative permeability model (see Eq. (19)) assumes that k_{ra} is a unique function of \bar{S}_a^{aoiw} ($\bar{S}_a^{aoiw} = 1 - \bar{S}_l^{aoiw}$) and independent of ϕ_{soiw} . Fig. 7 shows the calculated values of k_{ra} as a function of \bar{S}_l^{aoiw} . Observe that increasing \bar{S}_l^{aoiw} leads to a decrease in k_{ra} owing to the reduction of pores accessible for air flow. The reported dependence of k_{ra} on the liquid saturations (Honarpour et al., 1986) has been attributed to air entrapment (Donaldson and Kayser, 1981), which is not incorporated in the presented model. Land (1968) and Lenhard and Parker (1987) present pore-size distribution permeability models which account for non-wetting fluid entrapment. These hysteretic models also may be revised to account for wettability. The details of this modification are not discussed herein owing to the more speculative nature of such a model.

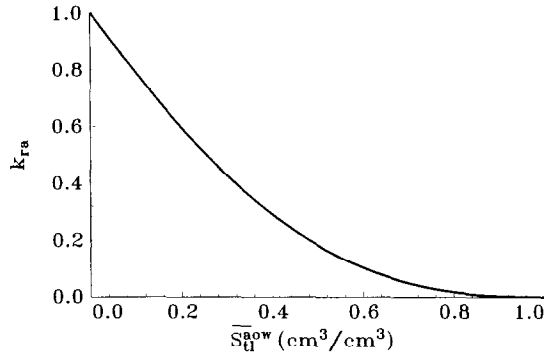


Fig. 7. Calculated values of k_{ra} according to Eq. (19) as function of \bar{S}_{oi}^{aow} .

The behavior of three-phase systems having saturation-dependent wettability is similar to that presented above. Increasing the organic-wet fraction leads to a greater k_{rw} and a smaller k_{ro} for given saturations, and k_{rw} and k_{ro} are functions of both water and oil saturations. In contrast, the magnitude of k_{rw} and k_{ro} also depends on the saturation dependency of ϕ_{sow} . As for the two-fluid system (see Fig. 4) the saturation dependency of ϕ_{sow} is more pronounced for media having larger organic-wet fractions.

4. Evaluation

Although experimental two- and three-fluid k_r - S relations have previously been measured, these data are generally inadequate to compare quantitatively with the estimation procedure presented herein, since the methodology requires P_c - S data as well as contact angles. Donaldson and Thomas (1971) measured organic-water k_r - S relations for Torpedo sandstone having various degrees of fractional wettability; wettability alterations were achieved by treating the cores with different concentrations of organochlorosilane. Fig. 8(a) presents their measured k_{ro} - \bar{S}_w^{ow} relations. Here $\bar{S}_w^{ow} = (S_w^{ow} - S_{rw}^{ow}) / (1 - S_{rw}^{ow})$ with S_{rw}^{ow} set equal to the water saturation at the start of the experiment. These researchers determined the wettability of the cores according to the United States Bureau of Mines wettability index (I_{usbm}) (Donaldson et al., 1969). Higher values of I_{usbm} indicate a larger water-wet fraction. Note that, in general, k_{ro} decreases at a given \bar{S}_w^{ow} with decreasing I_{usbm} . The exception to this trend is that the value of k_{ro} for $I_{usbm} = 0.649$ is slightly lower than that for $I_{usbm} = 0.179$. It is hypothesized herein that this may be due to slight differences in the pore-size distribution between the cores, or errors in the measurement of \bar{S}_w^{ow} . Since P_c - S data for these Torpedo sandstone cores were not presented in the literature, the direct estimation of these k_{ro} - \bar{S}_w^{ow} relations is not possible.

To qualitatively assess the utility of the predictive procedure presented in this work the value of m from the analytical solution of the Burdine model (cf. van Genuchten et al., 1991) was fitted to the measured k_{ro} - \bar{S}_w^{ow} data for $I_{usbm} = -1.333$ (the system which was the most strongly wetted, in this case by organic) shown in Fig. 8(a). This fitted value of $m = 1 - 2/n = 0.4629$ was used to predict the corresponding P_c - S curve

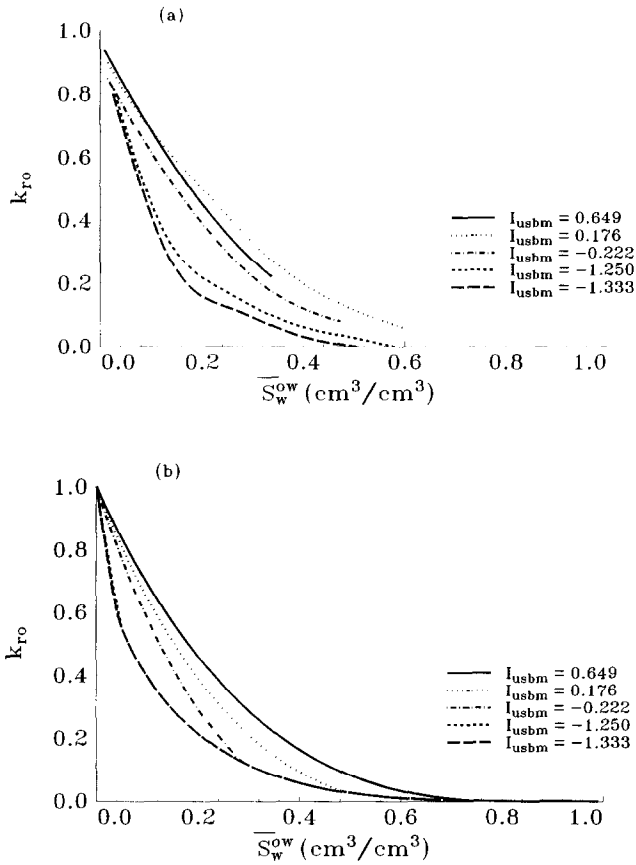


Fig. 8. (a) and (b). Measured and predicted $k_{ro} - \bar{S}_w^{ow}$ relations for variously wetted Torpedo sandstone containing brine and Squirrel crude oil. Measured data are from Donaldson and Thomas (1971).

(van Genuchten, 1980): Here an $\alpha_d = 0.02536$ ($\alpha_i = 2\alpha_d$) parameter was estimated from the reported mean pore size of Torpedo sandstone ($11.5 \mu\text{m}$) (Singh, 1990) and the reported interfacial tension of Squirrel crude oil ($\sigma_{ow} = 0.0223 \text{ N m}^{-1}$) (Donaldson et al., 1969). Hypothetical $P_c - S$ curves for the different wettabilities were obtained by shifting the previously estimated $P_c - S$ curve downward until the appropriate I_{usbm} wettability index was achieved (see Bradford and Leij, 1996). Values for $\phi_{sow}(\bar{S}_w^{ow})$ were then calculated from these estimated $P_c - S$ curves according to Eq. (16); $P_{ao} - \bar{S}_o^{ao}$ data were replaced by the estimated $P_c - S$ curve for the perfectly wetted system. Fig. 8(b) shows the resultant estimated $k_{ro} - \bar{S}_w^{ow}$ relations which correspond to the measured data shown in Fig. 8(a). Note that Fig. 8(b) captures the general trends shown in Fig. 8(a); increasing the organic-wet fraction leads to a decrease in k_{ro} at a given saturation. The influence of wettability on the measured $k_{ro} - \bar{S}_w^{ow}$ relations is less marked than that predicted in Fig. 8(b). This discrepancy may be due to inaccuracies in the estimation of S_{rw}^{ow} or the $\phi_{sow}(\bar{S}_w^{ow})$ relations.

5. Summary and conclusions

Two- and three-fluid k_r - S relations are required to simulate multiphase flow and transport processes. Commonly, these permeability relations are estimated from more widely available P_c - S data according to statistical pore-size distribution models. Previous pore-size distribution models, however, are based on restrictive wettability assumptions. A modification of the Burdine pore-size distribution model is presented herein to estimate two- and three-fluid k_r - S relations for media having non-zero contact angles and/or fractional wettability.

For two-fluid systems, descriptions of the wetting and non-wetting fluid permeability were combined for both water and organic phases. The contributions of wetting and non-wetting pore classes to k_{rw} and k_{ro} were determined based on wettability. A constant weighting function given by Eq. (15) was proposed for non-zero contact angles. The weighting function will be a function of saturation for fractional wettability media. The resultant permeability model predicts that a greater contact angle or organic-wet fraction will lead to an increase in k_{rw} and a decrease in k_{ro} at a given saturation.

For three-fluid systems organic and water were assumed to be distributed in small and medium pore classes, while air was assumed to reside entirely in pores belonging to the ‘largest’ pore class. The permeability of water and organic were represented, thus, as composites of wetting and intermediate fluid pore classes. The contribution of a particular pore class was again determined by wettability. Behavior at the wettability extremes is preserved by the model, while k_{rw} and k_{ro} are functions of both \bar{S}_o^{aow} and \bar{S}_w^{aow} for $0^\circ < \phi_{sow} < 180^\circ$. The permeability to a particular fluid (i.e. k_{rw} , k_{ro} , and k_{ra}) mainly depends upon that fluid’s saturation (\bar{S}_w^{aow} , \bar{S}_o^{aow} , and \bar{S}_a^{aow} , respectively) since this saturation determines the number of pores accessible for flow. The model predicts k_{rw} will increase and k_{ro} will decrease at a given saturation for a greater ϕ_{sow} and/or organic-wet fraction. The value of k_{ra} was assumed to be independent of wettability and uniquely a function of the total liquid saturation.

This paper attempts to predict the influence of wettability on k_r - S relations. Comparison with available data suggests that the presented model captures the general trends reported in the literature for wettability effects on two-fluid k_r - S relations (Owens and Archer, 1971; McCaffery and Bennion, 1974). Furthermore, the conceptual model for three-fluid k_r - S relations provides predictions consistent with observed differences in the saturation dependency of relative permeabilities (Honarpour et al., 1986). Additional experimental studies are required to further evaluate and refine the modelling approach.

6. Notation

a	air
A_{kl}^*	interfacial area per unit pore volume between phases k and l ($\text{cm}^2 \text{cm}^{-3}$)
A_s	solid surface area per unit bulk volume ($\text{cm}^2 \text{cm}^{-3}$)
A_s^*	solid surface area per unit pore volume ($\text{cm}^2 \text{cm}^{-3}$)
A_{se}^*	effective solid surface area per unit pore volume ($\text{cm}^2 \text{cm}^{-3}$)

C_k	Kozeny constant
f	weighting function
F_o	organic wet fraction
g	acceleration owing to gravity (m s^{-2})
H	hydraulic head (cm)
I_{usbm}	United States Bureau of Mines (usbm) wettability index
k_r	relative permeability
k_{rp}	relative permeability of phase p
o	organic
P_c	capillary pressure (N m^{-2} , cm water)
P_p	pressure of phase p (N m^{-2} , cm water)
P_{kl}	capillary pressure drop over interface between fluids k and l , i.e. $P_k - P_l$ (N m^{-2} , cm water)
q_i	flux of through i th capillary tube (cm s^{-1})
r_h	hydraulic radius (cm)
R	radius of a capillary tube (cm)
s	solid
S	saturation ($\text{cm}^3 \text{cm}^{-3}$)
S_{ik}^{ik}	“immobile” residual wetting fluid saturation of fluid k ($\text{cm}^3 \text{cm}^{-3}$)
S_k^{kl}	saturation of fluid k in a medium containing the two fluids k and l ($\text{cm}^3 \text{cm}^{-3}$)
S_k^{klm}	saturation of fluid k in a medium containing the three fluids k , l , and m ($\text{cm}^3 \text{cm}^{-3}$)
S_{mkt}^{mkt}	saturation of maximum entrapped fluid k ($\text{cm}^3 \text{cm}^{-3}$)
S_r	residual saturation ($\text{cm}^3 \text{cm}^{-3}$)
S_{tl}	total liquid saturation ($\text{cm}^3 \text{cm}^{-3}$)
\bar{S}	effective saturation ($\text{cm}^3 \text{cm}^{-3}$)
w	water
ε	porosity ($\text{cm}^3 \text{cm}^{-3}$)
μ	viscosity of the fluid (g cm^{-1})
ρ	density of the fluid (g cm^{-3})
σ_{kl}	interfacial tension at interface between fluids k and l (N m^{-1})
ϕ_{skl}	equilibrium contact angle at contact line between solid and fluids i and j (degree)
ϕ_{skl}^{\wedge}	advancing contact angle (degree)
ϕ_{skl}^{R}	receding contact angle (degree)

Acknowledgements

Funding for this research was provided by the National Institute of Environmental Health Sciences under Grant # ES04911. Partial funding for this research was also provided by the National Science Foundation under Grant # EID9023090, and by the Department of Energy under Grant # DE-FG07-96ER14702. The research described in

this article has not been subject to Agency review and, therefore, does not necessarily reflect the views of the Agency, and no official endorsement should be inferred.

Appendix A

Throughout this paper effective saturations have been used to quantify the pore space accessible for flow. For organic–water systems, the effective water saturation is defined as:

$$\bar{S}_w^{\text{ow}} = \frac{S_w^{\text{ow}} - S_{iw}^{\text{ow}}}{1 - S_{iw}^{\text{ow}} - S_{io}^{\text{ow}}} \quad (\text{A1})$$

Similarly the effective organic saturation is given as:

$$\bar{S}_o^{\text{ow}} = \frac{S_o^{\text{ow}} - S_{io}^{\text{ow}}}{1 - S_{iw}^{\text{ow}} - S_{io}^{\text{ow}}} \quad (\text{A2})$$

where S_{iw}^{ow} and S_{io}^{ow} are the “immobile” residual water and organic saturations, respectively, expressed as volume of fluid per volume of pore space. In a three-fluid system the effective water and organic saturations are defined analogously to Eqs. (A1) and (A2), respectively; where the superscript ow is now replaced by aow. The effective air saturation is given as:

$$\bar{S}_a^{\text{aow}} = \frac{S_a^{\text{aow}}}{1 - S_{iw}^{\text{aow}} - S_{io}^{\text{aow}}} \quad (\text{A3})$$

The effective total liquid saturation (\bar{S}_l^{aow}) is equal to $1 - \bar{S}_a^{\text{aow}}$.

The lowest water (S_{rw}^{ow}) and organic (S_{ro}^{ow}) saturations may be determined from $P_{\text{ow}} - S_{vw}^{\text{ow}}$ data. For uniformly wetted medium with $0^\circ \leq \phi_{\text{sow}} < 90^\circ$, S_{io}^{ow} is zero and $S_{iw}^{\text{ow}} = S_{rw}^{\text{ow}}$. Analogously, S_{iw}^{ow} is zero for $90^\circ \leq \phi_{\text{sow}} \leq 180^\circ$ and $S_{io}^{\text{ow}} = S_{ro}^{\text{ow}}$. For fractional wettability media both S_{io}^{ow} and S_{iw}^{ow} may be non-zero owing to the presence of organic- and water-wet solids. In this case, it is assumed that $S_{io}^{\text{ow}} = S_{ro}^{\text{ow}} - S_{mot}^{\text{ow}}$ and $S_{iw}^{\text{ow}} = S_{rw}^{\text{ow}} - S_{mwt}^{\text{ow}}$, where S_{mot}^{ow} and S_{mwt}^{ow} are the maximum entrapped organic and water, respectively. The maximum amount of entrapped fluid is not known a priori for fractional wettability systems. It is hypothesized herein that an estimate of $\bar{S}_{mot}^{\text{ow}}$ may be obtained from scaling \bar{S}_{ra}^{ao} of an air–organic system by $\sigma_{\text{ow}}(1 - F_o)/\sigma_{\text{ao}}$ (see Bradford and Leij, 1997); where F_o is the mass fraction of organic-wet solids. Similarly, an estimate of $\bar{S}_{mwt}^{\text{ow}}$ may be obtained by multiplying \bar{S}_{ra}^{ao} by $\sigma_{\text{ow}}F_o/\sigma_{\text{ao}}$. Note that $\bar{S}_{mot}^{\text{ow}}$ and $\bar{S}_{mwt}^{\text{ow}}$ are associated with the water-wet ($1 - F_o$) and organic-wet (F_o) fractions, respectively. Bradford and Leij (1997) discuss a method for determining F_o for a fractional wettability medium.

References

- Anderson, W.G., 1986. Wettability literature survey—Part 2: wettability measurement. *Journal of Petroleum Technology* Nov. 38, 1246–1261.

- Anderson, W.G., 1987a. Wettability literature survey—Part 4: effects of wettability on capillary pressure. *Journal of Petroleum Technology* Oct. 39, 1283–1299.
- Anderson, W.G., 1987b. Wettability literature survey—Part 5: the effects of wettability on relative permeability. *Journal of Petroleum Technology* Nov. 39, 1453–1467.
- Bradford, S.A., Leij, F.J., 1995a. Wettability effects on scaling two- and three-fluid capillary pressure–saturation relations. *Environmental Science and Technology* 29, 1446–1455.
- Bradford, S.A., Leij, F.J., 1995b. Fractional wettability effects on two- and three-fluid capillary pressure–saturation relations. *Journal of Contaminant Hydrology* 20, 89–109.
- Bradford, S.A., Leij, F.J., 1996. Predicting two- and three-fluid capillary pressure–saturation relations in mixed wettability media. *Water Resources Research* 32, 251–259.
- Bradford, S.A., Leij, F.J., 1997. Estimating interfacial areas for multi-fluid soil systems. *J. Contam. Hydrol.* 27, 83–105.
- Brown, R.J.S., Fatt, I., 1956. Measurements of fractional wettability of oilfield rocks by the nuclear magnetic relaxation method. *Transactions of the American Institute of Mining, Metallurgical and Petroleum Engineers* 207, 262–264.
- Burdine, N.T., 1953. Relative permeability calculations from pore-size distribution data. *Transactions of the American Institute of Mining, Metallurgical and Petroleum Engineers* 198, 71–77.
- Carman, P.C., 1937. Fluid flow through a granular bed. *Transactions of the Institute of Chemical Engineers* 23, 150–156.
- Caudle, B.H., Slobod, R.L., Brownscombe, E.R., 1951. Further developments in the laboratory determination of relative permeability. *Transactions of the American Institute of Mining, Metallurgical and Petroleum Engineers* 192, 145–150.
- Corey, A.T., Rathjens, C.H., Henderson, J.H., Wyllie, M.R.J., 1956. Three-phase relative permeability. *Transactions of the American Institute of Mining, Metallurgical and Petroleum Engineers* 207, 349–351.
- Dekker, L.W., Ritsema, C.J., 1994. How water moves in a water repellent sandy soil. 1. potential and actual water repellency. *Water Resources Research* 30, 2507–2519.
- Demond, A.H., Desai, F.N., Hayes, K.F., 1994. Effect of cationic surfactants on organic liquid–water capillary pressure–saturation relationships. *Water Resources Research* 30, 333–342.
- Demond, A.H., Rathfelder, K., Abriola, L.M., 1996. Simulation of organic liquid flow in porous media using estimated and measured transport properties. *Journal of Contaminant Hydrology* 22 (3–4), 223–240.
- Demond, A.H., Roberts, P.V., 1993. Estimation of two-phase relative permeability relationships for organic liquid contaminants. *Water Resources Research* 4, 1081–1090.
- Donaldson, E.C., Dean, G.W., 1966. Two- and three-phase relative permeability studies. U.S. Bureau of Mines, Report #6826. Washington, D.C.
- Donaldson, E.C., Kayser, M.B., 1981. Three-phase flow in porous media. DOE/BETC/IC–80/4.
- Donaldson, E.C., Thomas, R.D., 1971. Microscopic observations of oil displacement in water-wet and oil-wet systems. SPE paper # 3555, SPE Annual Meetings, New Orleans, LO.
- Donaldson, E.C., Thomas, R.D., Lorenz, P.B., 1969. Wettability determination and its effect on recovery efficiency. *Society of Petroleum Engineers Journal* March 9, 13–20.
- Dria, D.E., Pope, G.A., Sepehrmoori, K., 1993. Three-phase gas/oil/brine relative permeabilities measured under CO₂ flooding conditions. *SPE Reservoir Engineering* May 8, 143–150.
- Fatt, I., Klikoff, W.A. Jr., 1959. Effect of fractional wettability on multiphase flow through porous media. *Transactions of the American Institute of Mining, Metallurgical and Petroleum Engineers* 216, 426–429.
- Heaviside, J., Brown, C.E., Gamble, I.J.A., 1987. Relative permeability for intermediate wettability reservoirs. SPE paper # 16968. Dallas, TX.
- Honarpour, M., Koederitz, L., Harvey, A.H., 1986. *Relative Permeability of Petroleum Reservoirs*. CRC Press.
- Klute, A., Dirksen, C., 1986. Hydraulic conductivity and diffusivity: laboratory methods. In: Klute, A. (Ed.) *Methods of Soil Analysis, Part 1, Physical and Mineralogical Methods*. 2nd ed. American Society of Agronomy, Madison, WI.
- Land, C.S., 1968. Calculation of imbibition relative permeability for two- and three-phase flow from rock properties. *Society of Petroleum Engineers Journal* June 8, 149–156.
- Laplace, P.S., 1825. *Traite de Mechanique Celeste*, Chez J.B.M. Duprat. Paris.
- Lenhard, R.J., Parker, J.C., 1987. A model for hysteretic constitutive relations governing multiphase flow 2. Permeability–saturation relations. *Water Resources Research* 23, 2197–2206.

- Leverett, M.C., Lewis, W.B., 1941. Steady flow of gas–oil–water mixtures through unconsolidated sands. *Transactions of the American Institute of Mining, Metallurgical and Petroleum Engineers* 142, 107–117.
- Marquardt, D.W., 1963. An algorithm for least-squares estimation of nonlinear parameters. *Journal of the Society for Industrial and Applied Mathematics* 11, 431–441.
- McCaffery, F.G., Bennion, D.W., 1974. The effect of wettability on two-phase relative permeabilities. *Journal of Canadian Petroleum Technology* 13, 42–53.
- Morrow, N.R., 1970. Physics and thermodynamics of capillary action in porous media. In: de Wiest, Roger J.M. (Ed.), *Flow Through Porous Media*, Academic Press.
- Morrow, N.R., 1975. The effects of surface roughness on contact angle with special reference to petroleum recovery. *Journal of Canadian Petroleum Technology* Oct.–Dec. 14, 42–53.
- Morrow, N.R., 1976. Capillary pressure correlations for uniformly wetted porous media. *Journal of Canadian Petroleum Technology* Oct.–Dec. 15, 49–69.
- Morrow, N.R., 1990. Wettability and its effect on oil recovery. *Journal of Petroleum Technology* 42, 1476–1484.
- Morrow, N.R., Cram, P.J., McCaffery, F.G., 1973. Displacement studies in Dolomite with wettability control by octanoic acid. *Society of Petroleum Engineers Journal* August 13, 221–232.
- Morrow, N.R., McCaffery, F.G., 1978. Displacement studies in uniformly wetted porous media. In Padday, J.F. (Ed.), *Wetting, Spreading and Adhesion*. Academic Press.
- Mualem, Y., 1976. A new model for predicting the hydraulic conductivity of unsaturated porous media. *Water Resources Research* 12, 513–522.
- Oak, M.J., Baker, L.E., Thomas, D.C., 1990. Three-phase relative permeability of Berea sandstone. *Journal of Petroleum Technology* August 42, 1054–1061.
- Owens, W.W., Archer, D.L., 1971. The effect of rock wettability on oil–water relative permeability relationships. *Journal of Petroleum Technology* July 23, 873–878.
- Powers, S.E., Tamblin, M.E., 1995. Wettability of porous media after exposure to synthetic gasolines. *Journal of Contaminant Hydrology* 19, 105–125.
- Rapoport, L.A., Leas, W.J., 1951. Relative permeability to liquid in liquid–gas systems. *Transactions of the American Institute of Mining, Metallurgical and Petroleum Engineers* 192, 83–95.
- Reid, S., 1958. The flow of three immiscible fluids in porous media. PhD Dissertation, Chemical Engineering Dept., University of Birmingham, UK.
- Salathiel, R.A., 1973. Oil recovery by surface film drainage in mixed wettability rocks. *Journal of Petroleum Technology* Oct. 25, 1216–1224.
- Saraf, D.N., Fatt, I., 1967. Three-phase relative permeability measurement using a nuclear magnetic resonance technique for estimating fluid saturation. *Society of Petroleum Engineers Journal* Sept. 7, 235–242.
- Sarem, A.M., 1966. Three-phase relative permeability measurements by unsteady-state method. *Society of Petroleum Engineers Journal* Sept. 6, 199–205.
- Singh, B., 1990. Capillary Pressure Phenomena in Porous Media. MS Thesis, Dept. of Petroleum Engineering, University of Oklahoma, Norman, OK.
- Soil Survey Staff. 1975. *Soil Taxonomy: a basic system of soil classification for making an interpreting soil surveys*. USDA-SCS Agricultural Handbook 436. U.S. Government Printing Office, Washington, DC.
- Snell, R.W., 1962. Three-phase relative permeability in an unconsolidated sand. *Journal of the Institute of Petroleum* 48, 80–88.
- van Genuchten, M.Th., 1980. A closed form equation for predicting the hydraulic conductivity of unsaturated soils. *Soil Science Society of America Journal* 44, 892–898.
- van Genuchten, M. Th., Leij, F.J., Yates, S.R., 1991. The RETC code for quantifying the hydraulic functions of unsaturated soils. EPA/600/2–91/065.